Commun. Theor. Phys. **76** (2024) 095405 (12pp) https://doi.org/10.1088/1572-9494/ad5718

Thermal analysis of the Rindler–Schwarzschild black hole via corrected entropy

Allah Ditta[1], **Xia Tiecheng**[1], **Riasat Ali**[1] **and Ali Övgün**[2,*]

[1] Department of Mathematics, Shanghai University and Newtouch Center for Mathematics of Shanghai University, Shanghai, 200444, China
[2] Physics Department, Eastern Mediterranean University, Famagusta, 99628 North Cyprus via Mersin 10, Turkiye

E-mail: mradshahid01@gmail.com, xiatc@shu.edu.cn, riasatyasin@gmail.com and ali.ovgun@emu.edu.tr

Received 2 February 2024, revised 2 June 2024
Accepted for publication 5 June 2024
Published 24 July 2024

Abstract

In this study, we investigate the thermodynamic characteristics of the Rindler–Schwarzschild black hole solution. Our analysis encompasses the examination of energy emission, Gibbs free energy, and thermal fluctuations. We calculate various quantities such as the Hawking temperature, geometric mass, and heat capacity to assess the local and global thermodynamic stability. The temperature of the black hole is determined using the first law of thermodynamics, while the energy emission rate is evaluated as well. By computing the Gibbs free energy, we explore the phase transition behavior exhibited by Rindler–Schwarzschild black hole, specifically examining the swallowing tails. Moreover, we derive the corrected entropy to investigate the influence of thermal fluctuations on small and large black holes. Notably, we compare the impact of correction terms on the thermodynamic system by comparing the results obtained for large black holes and small black holes.

Keywords: black holes, thermodynamics, thermal fluctuations, heat capacity, Gibbs free energy, energy emission, Rindler–Schwarzschild black hole

(Some figures may appear in colour only in the online journal)

1. Introduction

Black hole thermodynamics are a fascinating field that bridge the classical and quantum facets of gravity. While essentially quantum in nature, a black hole's (BHs) thermodynamic properties, such as entropy and temperature, correspond to more regular features like surface gravity and horizon size [1–5]. In fact, Bardeen, Carter, and Hawking's significant study made the connection between BH fluctuations and the first law of thermodynamics by taking into account the usual reaction of a BH to infalling matter [6]. The explanation of the different variables and our knowledge of BH thermodynamics have both advanced recently. By incorporating pressure under the guise of deviations in vacuum energy, the laws of thermodynamics in gravitational mechanisms have been more thoroughly understood as an extended thermodynamical law [7–12, 87–91] and a more precise description of the BH physics has made the mass apparent as its enthalpy.

These efforts to comprehend the First Law have mainly focused on BHs, such as those found in the solutions of the Kerr–Newman family. However, there are multi-BH systems with known, precise solutions that are more fascinating. This makes such geometries suitable for thermodynamic analysis. For instance, the Israel–Khan solution [13] is an asymptotically flat structure made up of two BHs that are separated from one another by a 'strut,' which is a conical defect with an angular excess, that corresponds to a cosmic string with negative tension. More generally, by extending a positive-tension cosmic string through spacetime, one can give up global asymptotic flatness in order to fix the unphysical

* Author to whom any correspondence should be addressed.

negative-tension defect [14–16]. One preserves the local asymptotic flat away from the core by doing this. Further generalising, the accelerating BH contained in the C-metric [17, 18] is made up of a BH and a cosmic string that extends [19, 20] from it as it generates an accelerating force.

A non-compact acceleration horizon also develops in this situation, in addition to asymptotic flatness being lost near the string's extension to spatial infinity. A fixed deficiency threading the horizon or an insufficient variation during the absorption [21] of a cosmic string were the main topics of early thermodynamic studies of BH conical defects [22–25]. However, it has only recently been determined what a truly changing delay would mean in terms of thermodynamics. In particular, an asymptotically local anti-de Sitter BH that is accelerating has given rise to a situation where one can maintain fantastic computation efficiency. There has also been some progress in understanding the origin of thermodynamic length. Krtous and Zelnikov [26] discovered a thermodynamic length corresponding to the strut world volume evaluated at a specific time when considering the two BHs coupled by a strut. For similarly coupled Kerr–Newman BHs, this has since been confirmed [27].

Entropy and Bekenstein's area are associated [1, 28] with studying the thermodynamics of BH, and the thermodynamics law can be used to calculate temperature. The corrected BH thermodynamics can be used to study many significant properties of BH, such as unstable and stable forms, criticality, holographic duality and multiple critical perspectives. The quantum-corrected fluctuations in BH thermodynamics have taken on a significant role in the study of the physics of BHs. The logarithmic correction effect of thermal fluctuations for charged anti-de Sitter BH, Horava–Lifshitz BH and Kerr-AdS BH has been calculated by Pourhassan *et al* [29–31]. The corrected entropy corrections for spinning BHs, Reissner–Nordstrom, Kerr, charged AdS BHs and other types of BHs have been studied by Faizal and Khalil [32]. They have also examined their remnants. For the Godel BH, the logarithmic modified entropy has been examined using the Cardy formula [33, 34] as well. Consideration of Kerr–Newman-anti-de Sitter and Reissner–Nordstrom's BHs of 1st-order modifications to temperature and entropy has been investigated to see how the modified temperature and entropy affect anti-de Sitter BH effects on thermodynamic parameters such as internal energy, enthalpy, Helmholtz energy and Gibbs free energy [35]. In modified Hayward-BHs thermodynamics [36], the impacts of thermal fluctuations have been studied. The impact of these modification terms on thermodynamic parameters such as inner energy, pressure, entropy and specific heat has been calculated [37].

The main goal of this study is to examine the effects of the Rindler parameter and the cosmological constant on the Hawking radiation. However, the BHs are surrounded by a dilaton field and the effects of the correction parameter, the Rindler parameter, and the cosmological constant may have important contributions to thermodynamics. Moreover, we investigate the significant scales that simulate the gravity of a central object, as well as a cosmic constant and Rindler parameter, which is a term that establishes the physical scales and subleading terms to the leading order in the significant radius expansion. With the exception of the Rindler term, general relativity also predicts all of these statements. Every realistic item passes through a transitional phase when it transitions from an unstable to a stable state, as indicated by Gibbs free energy and heat capacity transmission from a negative to a positive area. Heat capacity dissipation reveals the crucial points for phase transition.

We proceed with our study in this manuscript in the following scheme: in section 2, we explain the brief review of Rindler–Schwarzschild black hole. In section 3, we discuss the physical existence of BH by explaining the geometric mass and Hawking temperature. In section 4, we study the corrected entropy. In section 5, we study the thermal stability of BH by discussing the heat capacity and Gibbs free energy. Section 6, discusses the emission energy process of BH. In the last section 7, we write a brief summary of our concluding remarks.

2. Introductory review of the Rindler–Schwarzschild black hole

Assume a four-dimensional symmetric spherically line element defines spacetime [38] as

$$\mathrm{d}s^2 = f_{\mu\nu}\mathrm{d}x^\mu \mathrm{d}x^\nu + \Xi^2(\sin^2\theta \mathrm{d}\phi^2 + \mathrm{d}\theta^2). \tag{1}$$

In classical dynamics, the two-dimensional theory of equations of motion (EOM) leads to a four-dimensional metric (1) for every line element solution. The test particles are then considered to travel in the background of a four-dimensional metric (1). For further information, see [39]. The technique of spherical reduction [40] can reduce the four-dimensional Einstein–Hilbert action to a specific two-dimensional dilaton gravity model. This approach is novel in that it allows for infrared changes to the dilaton gravity model. The following assumptions are compatible with the general theory for two-dimensional geometry with field content f and Ξ. To begin, we assume that all non-renormalizable terms have been removed; therefore, the theory must be power-counting renormalizable. This precisely refers to the action [41, 42] as

$$S = -\frac{1}{k^2}\int \mathrm{d}^2x\sqrt{-f}[f(\Xi)R + 2(\partial\Xi)^2 - 2V(\Xi)]. \tag{2}$$

Consider an appropriate form for the kinetic term associated with the dilaton field Ξ via field redefinition. This assumption is not substantially dependent on the gravitational coupling constant (k). We assume that the free functions f and V are analytic in Ξ for large d, as in spherically omitted GR [39]. According to the EOM analysis, in order to reproduce the Newton potential ($-\frac{M}{r}$), the coupling function f that multiplies the Ricci scalar R must be supplied by $f=\Xi^2$ [43]. When $f=c\Xi^2$ is taken into account, the potential changes to $-\frac{M}{r^{1/c}}$ and $|c-1|<10^{-10}$ [44] is an observational bound for c. If the power of Ξ in the function f was modified, it would result in an exponential growth or decay of the potential. Further, we make the cautious assumption that $f=c\Xi^2$ is not

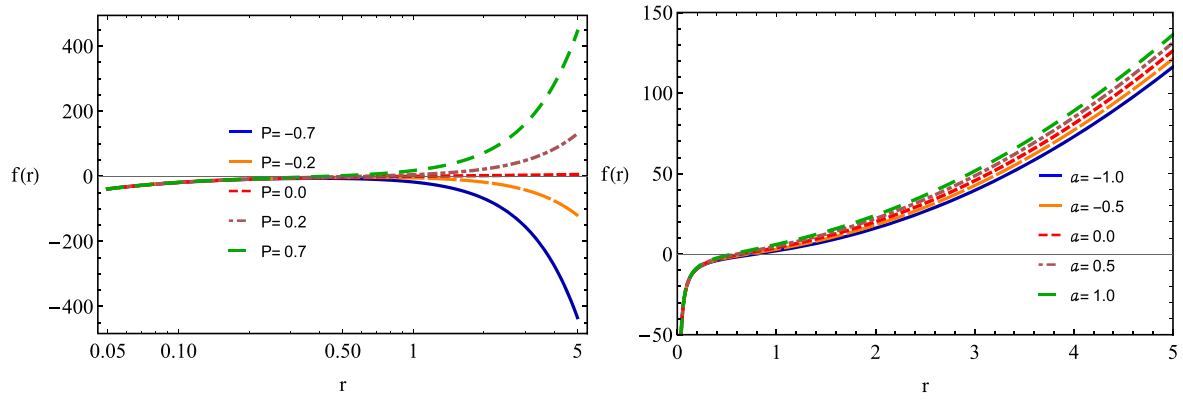

Figure 1. The figure shows the lapse function, $f(r)$, plotted against radius, r. Fixed parameters are $M = 1,\ P = 0.2,\ a = 0.5$.

renormalized in the infrared, which agrees perfectly with the experimental data. Choosing the possible V in the reaction (2) has to be done. In the four-dimensional structure words, we consider extensive surface regions surrounding a central item. At spherical reduction, the limit of an immense dilaton field (Ξ) follows the limit of enormous surface areas. We analyse the possibility of V performing in the following ways:

$$V(\Xi) = \Lambda\Xi^2 + a\Xi + b + O\left(\frac{1}{\Xi}\right). \tag{3}$$

Because the ansatz (3) for the potential V is critical to the discussion, let us take some time to explain its justification. Physics shows that the leading term Ξ in the huge expansion is quadratic, and that if we take permit powers bigger than Ξ^2, the resulting spacetime has a curvature singularity for large Ξ. As a result, the equation (3) is the universal asymptotic result requiring the absence of curvature singularity and analytic in Ξ in the infrared domain. With the impacts of the initial three terms in (3), the term $O(\frac{1}{\Xi})$ contributes to the gravitational potential in a proportionate way to $\ln r/r$. In the extreme infrared region, these effects are subordinate. As a result, we reject this sentence (along with other subleading phrases). We can fix the subleading coefficients in the asymptotic potential (3) by immediately re-scaling Ξ and k, which refers to setting up the physical length scale. We used $b = 2$ to preserve universality. The action (2) is reduced to eliminating all asymptotically subleading terms and selecting adequate normalisation of the coupling constants $k = 1$ as

$$S = -\int \mathrm{d}^2x\sqrt{-f}\,[\Xi^2 R + 2(\partial\Xi)^2 + 8a\Xi - 6\Lambda\Xi^2 + 2]. \tag{4}$$

It provides a generic, efficient theory of relativity in the infrared region that is consistent with the preceding conditions. The action (4) provides a theory whose existence depends upon the coupling constant a. The descending EOM solutions (4) are identified as a spherically symmetric solution (1) that model gravity in the infrared domain. It is easy to find solutions for the EOM [43] given as:

$$R = \frac{2}{\Xi} f^{\mu\nu}\Delta_\mu\partial_\nu\Xi - \frac{4a}{\Xi} - 6\Lambda, \tag{5}$$

$$f_{\alpha\beta}V(\Xi) = 2\Xi(\Delta_\alpha\partial_\beta - f_{\alpha\beta}\Delta^\mu\partial_\mu)\Xi - f_{\alpha\beta}(\partial\Xi)^2. \tag{6}$$

In [45–46], a spherically symmetric four-dimensional line element can be obtained as

$$\mathrm{d}s^2 = f(r)\mathrm{d}t^2 - \frac{\mathrm{d}r^2}{f(r)} - r^2(\sin^2\theta\mathrm{d}\phi^2 + \mathrm{d}\theta^2), \tag{7}$$

with

$$f(r) = 2ar - \frac{2M}{r} - \Lambda r^2 + 1 \ \textit{and}\ \ \Xi = r^2. \tag{8}$$

In equation (8), M is an integral constant related to the mass (AdM mass) of the Rindler–Schwarzschild black hole [45], and a is Rindler coupling parameter [43]. It is obvious that the considered spacetime transforms [45] into the well-known Schwarzschild BH for $a = 0 = \Lambda$. This study examines the geodesic evaluation of Grumiller's metric, which measures gravity over extended distances. The Rindler parameter can be compared to the Schwarzschild geodesic [47]. Furthermore, the Rindler–Schwarzschild black hole temperature was compared to the Schwarzschild BH in [48]. The black hole possesses Rindler parameter; hence, it is also known as the Rindler-improved Schwarzschild BH [49].

Here we choose $\Lambda = -8\pi P$ [50]. Here, pressure P is directly linked with the cosmological constant Λ, thus by taking the negative value of pressure we consider the anti-de Sitter spacetime (AdS-spacetime), and for positive values of P, we mean de Sitter spacetime (dS-spacetime) [51]. In this manuscript we analyze the black hole thermodynamics for both AdS-spacetime and dS-spacetime. The possible existence of positive and negative event horizons can be predicted by the physical behavior of lapse function $f(r)$ as shown in figure 1. It is obvious that for the fixed value of Rindler parameter a, positive pressure P depicts the positive event horizon and negative pressure P shows the negative event horizon along radial coordinate. For fixed positive pressure P, increasing values of a depict the increasing possibility of positive event horizon.

3. Physical existence of the Rindler–Schwarzschild black hole

The utilization of the lapse function provided by equation (8) to determine the mass of the BH confers significant importance. It signifies the presence of the BH in a physical sense.

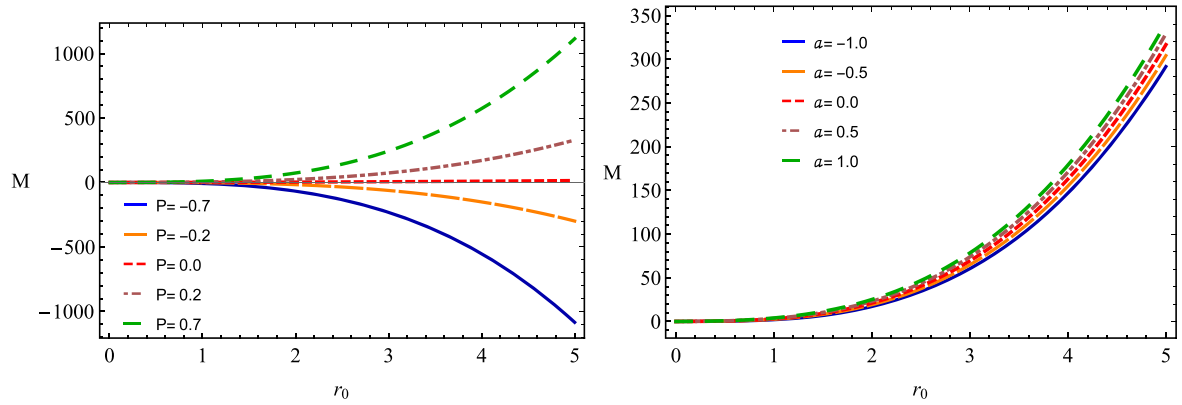

Figure 2. Geometric mass M and values of fixed parameters are $P = 0.2,\ a = 0.5$.

It is important to know that positive mass indicates stable BH, whereas negative mass indicates towards the instability of the BH. There are several approaches to calculating the mass of a black hole like the conformal approach [52–54], by using the first law of thermodynamics [55, 56]. Here, we calculate the geometric mass by setting $f(r) = 0$ [57, 58]. The ensuing equation furnishes the geometric mass of the BH, specifically in the context of our BH solution it is given as:

$$M = \frac{1}{2} r_0 (2ar_0 + 8\pi P r_0^2 + 1), \tag{9}$$

where r_0 is the BH horizon radius. We plot the geometric mass of the BH along horizon radius r_0 in figure 2. It is obvious that for the fixed value of Rindler parameter a, positive pressure P depicts the positive mass, and negative pressure P shows the negative mass along event horizon r_0. For fixed positive pressure P, increasing values of a depicted mass is positive. Thus pressure P and all values of a depict the stability of our solution of the Rindler–Schwarzschild BH.

The Hawking temperature T_H of the BH can be determined [59, 60] by $\frac{f'(r)}{4\pi}$ as:

$$T_H = \frac{a + \frac{M}{r_0^2} + 8\pi P r_0}{2\pi}. \tag{10}$$

The entropy of the BH can be written as [28]:

$$S = \pi r_0^2 \tag{11}$$

4. Corrected entropy

In this section, we investigate the impact of thermal fluctuations on the thermodynamics of the Rindler–Schwarzschild BH. To study this phenomenon, we utilize the formalism of Euclidean quantum gravity, which involves rotating the temporal coordinate within a complex plane. As a result, the partition function for the BH can mathematically be found in the references [61–66]. Specifically detailed calculations can be found in reference [62], where the simplified action is given as:

$$Z = \int DgDA \exp(-I), \tag{12}$$

where $I \to \iota\hat{I}$ is the Euclidean action of the field for this system, and the integral is taken over all fields that justify some periodicity or boundary condition. One can relate the statistical mechanical partition function [67, 68] as

$$Z = \int_0^\infty DE\Gamma(E)\exp(-\psi E), \tag{13}$$

where $\psi = T^{-1}$. We can calculate the density of states by using

$$\Gamma(E) = \frac{1}{2\pi i}\int_{\psi_0 - i\infty}^{\psi_0 + i\infty} d\psi e^{S(\psi)}, \tag{14}$$

where $S_c = \psi E + \ln Z$. The entropy near the equilibrium temperature ψ can be calculated by neglecting thermal fluctuations, which yields $S = \pi r_0^2$. But, when we are taking into account thermal fluctuations then the entropy $S_c(\psi)$ is given by [61]:

$$S_c = S + \frac{1}{2}(\psi - \psi_0)\left(\frac{\partial^2 S(\psi)}{\partial \psi^2}\right)_{\psi=\psi_0}. \tag{15}$$

So, one can write the density as stated by:

$$\Gamma(E) = \frac{1}{2\pi i}\int_{\psi_0 - i\infty}^{\psi_0 + i\infty} d\psi e^{\frac{1}{2}(\psi-\psi_0)\left(\frac{\partial^2 S(\psi)}{\partial \psi^2}\right)_{\psi=\psi_0}}, \tag{16}$$

which leads to

$$\Gamma(E) = \frac{e^S}{\sqrt{2\pi}}\left[\left(\frac{\partial^2 S(\psi)}{\partial \psi^2}\right)_{\psi=\psi_0}\right]^{\frac{1}{2}}. \tag{17}$$

We can write corrected entropy as

$$S_c = S - \frac{1}{2}\ln\left[\left(\frac{\partial^2 S(\psi)}{\partial \psi^2}\right)_{\psi=\psi_0}\right]^{\frac{1}{2}}. \tag{18}$$

The second derivative of entropy provides a measure of the squared fluctuation of energy. By utilizing the connection between conformal field theory and the microscopic degrees of freedom of a BH [69], it becomes possible to simplify this expression. Consequently, the entropy can be expressed as $S = m_1\psi^{n_1} + m_2\psi^{-n_2}$, where m_1, m_2, n_1, and n_2 are positive constants [34]. This entropy exhibits an extremum at

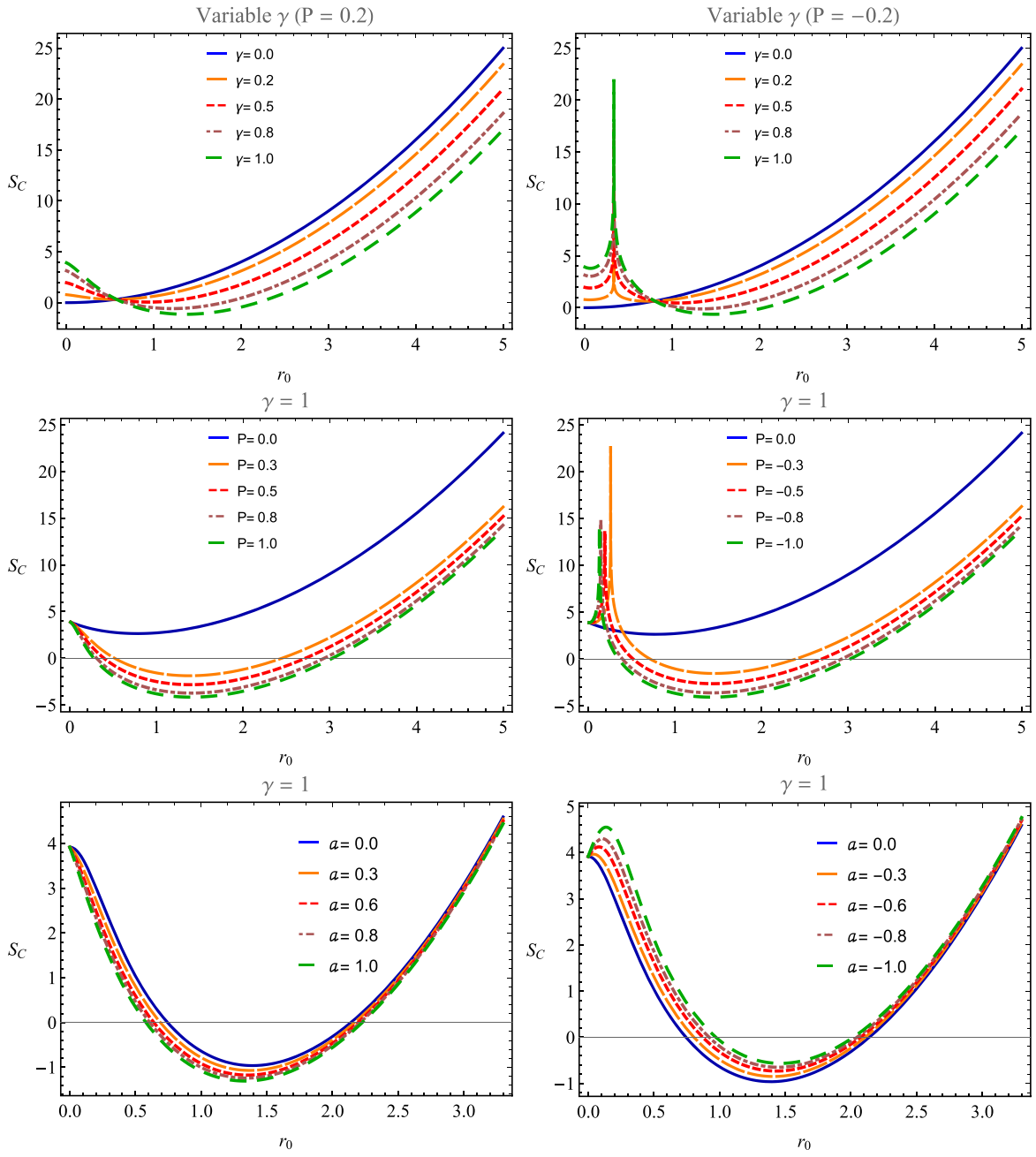

Figure 3. Corrected entropy S_C. Values of fixed parameters are $P = 0.2,\ a = 0.5$.

$\psi_0 = \left(\frac{mn_2}{m_1 n_1}\right)^{\frac{1}{n_1+n_2}} = T_H^{-1}$, where T_H denotes hawking temperature. By expanding the entropy around this extremum, we can determine [70, 71]:

$$\left(\frac{\partial^2 S(\psi)}{\partial \psi^2}\right)_{\psi=\psi_0} = S\psi_0^{-2}. \tag{19}$$

A corrected version of entropy by negating higher-order correction terms can be written as

$$S_c = S - \frac{1}{2}\ln ST_H^2. \tag{20}$$

Furthermore, the presence of quantum fluctuations in the geometry of BHs introduces a notable concern regarding thermal fluctuations in BH thermodynamics. These correction terms become significant when the size of the BH is small and its temperature is large. Hence, for large BHs, quantum fluctuations can be disregarded. It becomes evident that thermal fluctuations become significant solely for BHs characterized by high temperatures, and as the BH size decreases, its temperature increases. Thus, we can deduce that these correction terms are applicable solely to sufficiently small BHs exhibiting high temperatures [61]. Subsequently, we can derive the general expression for entropy by neglecting higher-order correction terms

$$S_c = S - \gamma \ln ST_H^2. \tag{21}$$

Here, we introduce γ as a constant parameter to incorporate

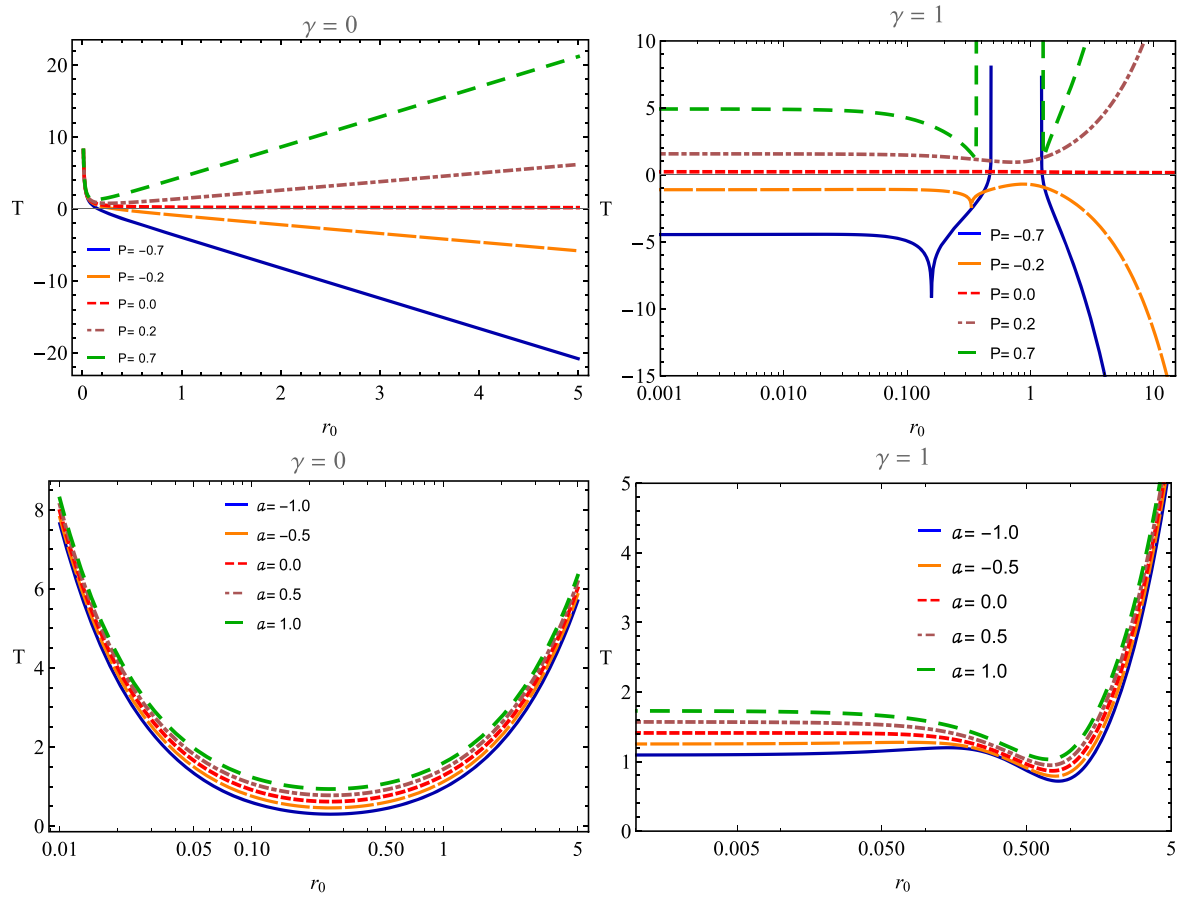

Figure 4. The figure shows temperature T versus the black hole horizon radius r_0. Fixed parameters are $P = 0.2,\ a = 0.5$.

the logarithmic correction terms associated with thermal fluctuations. By setting $\gamma = 0$, we recover the entropy without any correction terms As mentioned earlier, in the case of large BHs with extremely low temperatures, we can take $\gamma \to 0$, whereas, for small BHs with sufficiently high temperatures, we consider $\gamma \to 1$. By utilizing equations (10) and (21), we can obtain the following expression for the corrected entropy

$$S_c = \pi r_0^2 - \gamma \log\left(\frac{r_0^2\left(4a + \frac{24\pi P r_0^2 + 1}{\sqrt{r_0^2}}\right)^2}{16\pi}\right). \tag{22}$$

We plot S_C considering different choices of the correction parameter: $\gamma = 0$ for large black holes, $\gamma = 0.2$, 0.5, 0.8 & 1.0 for small black holes ($0 < \gamma < 1$), and $\gamma = 1$ for smaller black holes. The plot shown in figure 3 demonstrates that the entropy of spacetime consistently increases across the entire range considered for different values of γ with both positive and negative fixed values of pressure P. Moreover, for positive pressure, there is no fluctuation, while fluctuation can be observed for negative pressure. Notably, these fluctuations are more pronounced for smaller black holes. One can also observe an initial decrease in corrected entropy for different values of P & a by attaining the negative value, after that it increases continuously by maintaining the positive value. In the coming discussions, we calculate the other thermodynamic properties of BHs using this corrected entropy and compare the results by setting $\gamma = 0$ for no correction and $\gamma = 1$ for correction terms. Now, we determine the thermodynamic temperature T by using the first law of thermodynamics [55, 72]:

$$\mathrm{d}M = T\mathrm{d}S, \tag{23}$$

which yields the temperature as written below

$$T = \frac{-24\gamma P \log\left(\frac{(4a\sqrt{r_0^2} + 24\pi \mathrm{Pr}_0^2 + 1)^2}{16\pi}\right) + 24\pi \mathrm{Pr}_0^2 + 1}{4\sqrt{\pi}\sqrt{\pi r_0^2 - \gamma \log\left(\frac{(4a\sqrt{r_0^2} + 24\pi \mathrm{Pr}_0^2 + 1)^2}{16\pi}\right)}} + \frac{a}{\pi}. \tag{24}$$

For the next calculations, we incorporate the above calculated thermodynamic temperature T. We plot the temperature T in figure 4. One can see that in large BHs ($\gamma = 0$), for the fixed value of a and variable P, the BH is initially stable for small event horizon r_0 and afterward, for positive pressure the BH is globally unstable, whereas for negative pressure the BH is globally stable. For fixed pressure P and varying values of a. In small BHs ($\gamma = 1$), for the fixed value of a and variable P, the BH is unstable ($T < 0$) for positive pressure and the BH is stable ($T > 0$) for negative pressure. For the fixed values of P,

the BH is stable ($T>0$) in the case of both positive and negative a.

5. Thermal stability and phase transition

The thermal stability of the BH is examined by studying the behavior of the heat capacity C_P over both positive and negative intervals. Positive values of C_P signify the existence of a stable region, whereas negative values indicate an unstable region. Furthermore, the heat capacity plays a crucial role in interpreting phase transitions through its divergence [73–77]. In the case of the Rindler–Schwarzschild BH, the expression for the heat capacity can be represented as follows

$$\begin{aligned} C_P = & \frac{2(-4a\gamma\sqrt{r_0^2}+4\pi a(r_0^2)^{3/2}+24\pi^2Pr_0^4+\pi r_0^2(1-48\gamma P))}{C_1} \\ & \times\left[\pi r_0^2-\gamma\log\left[\frac{(4a\sqrt{r_0^2}+24\pi Pr_0^2+1)^2}{16\pi}\right]\right] \\ & \times\left[-24\sqrt{\pi}\gamma P\log\left[\frac{(4a\sqrt{r_0^2}+24\pi Pr_0^2+1)^2}{16\pi}\right]\right. \\ & +4a\sqrt{\pi r_0^2-\gamma\log\left[\frac{(4a\sqrt{r_0^2}+24\pi Pr_0^2+1)^2}{16\pi}\right]} \\ & \left.+24\pi^{3/2}Pr_0^2+\sqrt{\pi}\right], \end{aligned} \tag{25}$$

where

$$\begin{aligned} C_1 = & \sqrt{\pi}\sqrt{r_0^2}(4a(\pi r_0^2-\gamma)+\pi\sqrt{r_0^2}(24P(\pi r_0^2-2\gamma)+1)) \\ & \times\left[-24\gamma P\log\left[\frac{(4a\sqrt{r_0^2}+24\pi Pr_0^2+1)^2}{16\pi}\right]\right. \\ & \left.+24\pi Pr_0^2-1\right]. \end{aligned}$$

Figure 5 shows the heat capacity in small and large BHs. It can be identified that for large BHs ($\gamma=0$) in the case of variable pressure P, BHs shift the transition originally from unstable ($C_P<0$) to the globally stable region ($C_P>0$) for both positive and negative pressure, whereas for $P=0$ it shows the global instability ($C_P<0$). Also for variable a, BHs shift the transition from unstable ($C_P<0$ near event horizon r_0) to the stable region ($C_P>0$) for all values of a. In the case of smaller BHs ($\gamma=1$), the BHs show global stability ($C_P>0$) for small positive and negative values of P (i.e., $P=0.2,\ -0.2$), whereas for large positive and negative values of pressure P ($P=0.7,\ -0.7$), BHs are initially stable ($C_P>0$) then transit into the unstable region ($C_P<0$) and enter the globally stable region ($C_P>0$). And fixed pressure BHs are globally stable ($C_P>0$) for all values of a. If we talk about the phase transition points related to heat capacity for fix $a=0.5$ & $\gamma=0$: we observe singularity between $r_0=(0.142,\ 0.173)$ for $P=-0.7$, and $r_0=(0.317,\ 0.348)$ for $P=-0.2$, there is no phase transition for $p=0$. For $P=0.2$, the phase transition point lies between $r_0=(0.242,\ 0.274)$, and for $P=0.7$ the phase transition point lies between ($r_0=0.122,\ 0.154$). By fixing $a=0.5\ \gamma=1$, we get the following information: we observe singularity between $r_0=(0.003,\ 0.0345)$ for $P=-0.7$, and $r_0=(0.044,\ 0.076)$ for $P=-0.2$. There is no phase transition for $p=0$, and for $P=0.2$, the phase transition point lies between $r_0=(0.713,\ 0.745)$, and for $P=0.7$ phase transition point lies between $r_0=(0.35,\ 1.30)$. Then, by fixing $P=0.2\ \gamma=0$, we obtain the following information: the phase transition point for $a=-1$ is $r_0=0.25$. For $a=-0.5$, the phase transition point is $r_0=0.2575$. For $a=0.0$, the phase transition point is $r_0=0.257\,52$. For $a=0.5$, the phase transition point is $r_0=0.257\,516\,2$. For $a=1.0$, the phase transition point is $r_0=0.2576$. For fixing $P=0.2\ \gamma=1$, for all the selected values of a, $C_P>0$, thus shows no phase transition.

Figure 6 gives us information regarding the phase transition between large and small BHs. For $\gamma=0$ (Large BH), the temperature is low and for $\gamma=1$ (small BH), the temperature is high. Thus for negative pressure ($P=-0.7$), the critical point is $r_0=0.4$ where it shifts the transition between small and large BH. For positive pressure ($P=0.7$), the critical point is $r_0=0.325$ & 0.350, where it shifts the transition between small and large BHs.

Apart from heat capacity, the analysis of BH phase transitions also relies on the examination of Gibbs free energy. The Gibbs free energy exhibits unique features, including a 'swallowing tail', which assists in identifying the first-order phase transition point characterized by a discontinuity in its first-order derivative. Additionally, the continuous but non-smooth behavior of both the Gibbs free energy and its first-order derivative can indicate a second-order phase transition [78]. The computation of the Gibbs free energy can be performed using the formula [78] given as:

$$\begin{aligned} G=M-TS= & \frac{1}{2}r_0(2ar_0+8\pi Pr_0^2+1) \\ & -\left[\pi r_0^2-\gamma\log\left[\frac{(4a\sqrt{r_0^2}+24\pi Pr_0^2+1)^2}{16\pi}\right]\right] \\ & \times\left[\frac{-24\gamma P\log\left(\frac{(4a\sqrt{r_0^2}+24\pi Pr_0^2+1)^2}{16\pi}\right)+24\pi Pr_0^2+1}{4\sqrt{\pi}\sqrt{\pi r_0^2-\gamma\log\left(\frac{(4a\sqrt{r_0^2}+24\pi Pr_0^2+1)^2}{16\pi}\right)}}+\frac{a}{\pi}\right]. \end{aligned} \tag{26}$$

One can get detailed information about the phase transition points in both cases of larger BHs ($\gamma=0$) and smaller BHs ($\gamma=1$) through the graphical behavior of Gibbs free energy in figure 7.

6. Emission energy

Quantum fluctuations occurring within the interior of BHs results in the continual creation and annihilation of particles beyond the event horizon in large quantities. This tunneling phenomenon [79–83] causes positively charged particles to be attracted toward the innermost region of the BH, which leads to the emission of Hawking radiation and eventual evaporation of the BH over a specific period. The rate of

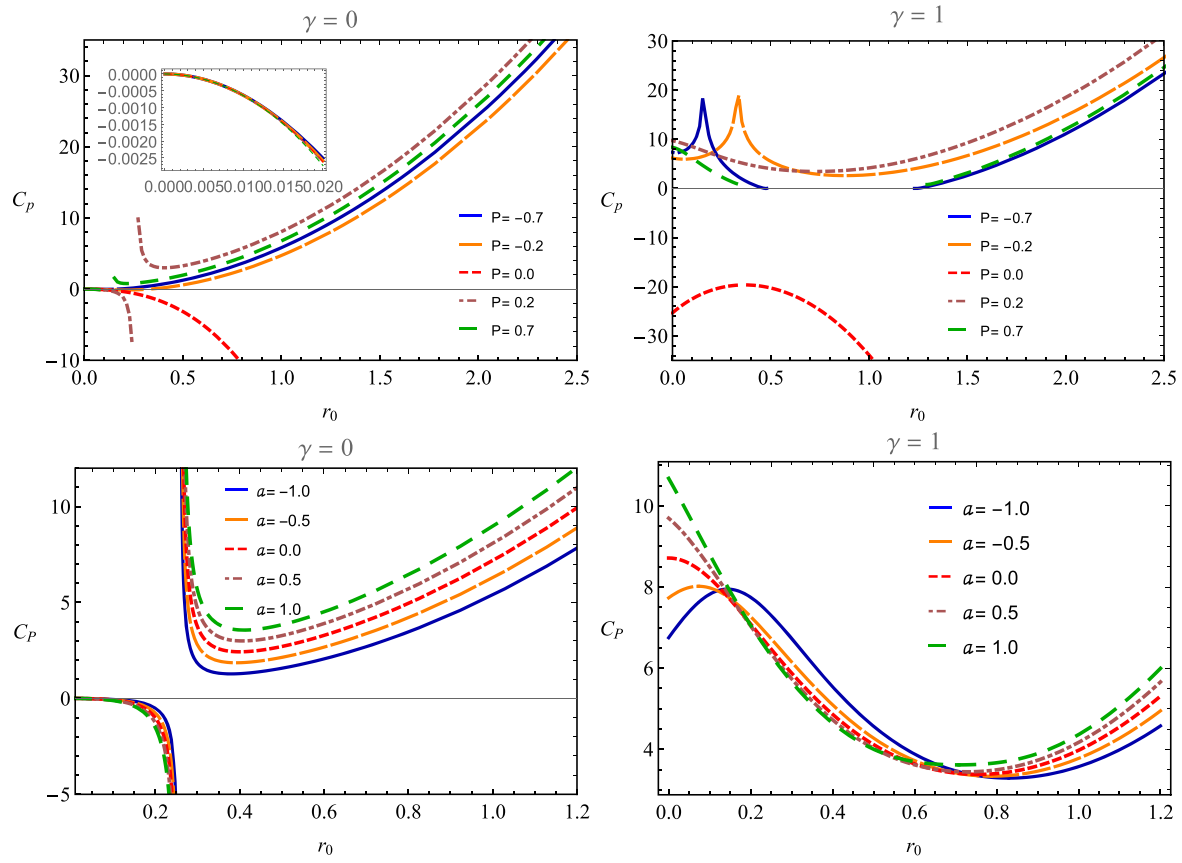

Figure 5. Heat capacity C_P. Values of fixed parameters are $P = 0.2,\ a = 0.5$.

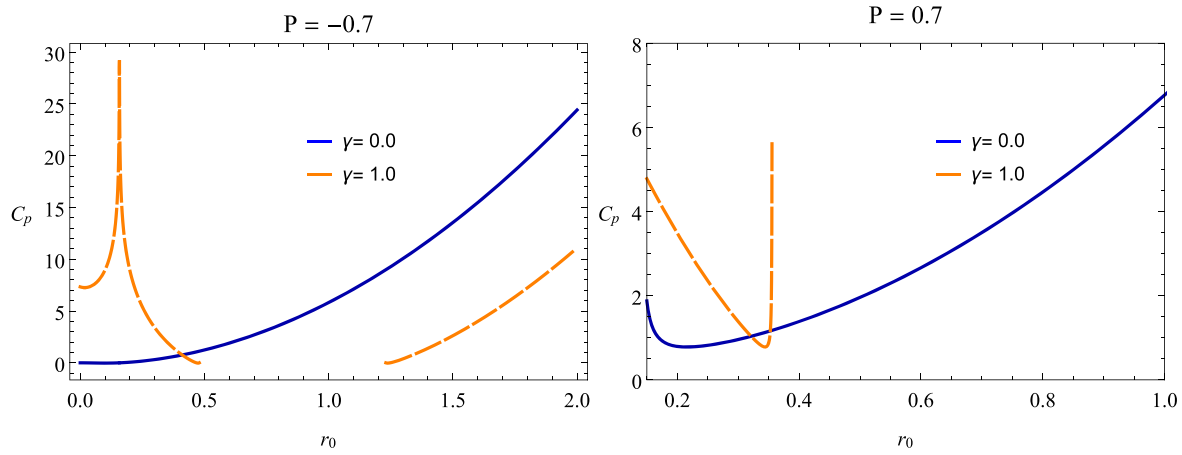

Figure 6. Heat capacity C_P for fixed constant $a = 0.5$.

evaporation is directly proportional to the energy emission rate. From the perspective of a distant observer, the high-energy reception cross-section closely approximates the BH shadow. This energy reception cross-section exhibits oscillations around a fixed, constrained value denoted as σ_{lim}, which corresponds to the radius of the BH [84–86]:

$$\sigma_{\rm lim} \approx \pi r_0^2, \tag{27}$$

where, r_0 is the event horizon radius of BH. Thus, the expression for the energy emission rate of BH is [85, 86]

$$\frac{{\rm d}^2\varepsilon}{{\rm d}\omega {\rm d}t} = \frac{2\pi^2\sigma_{\rm lim}}{{\rm e}^{\frac{\omega}{T}} - 1}\omega^3, \tag{28}$$

where, the temperature T is given in equation (24). One can get the expression for the emission energy process from equation (28) after replacing the horizon radius r_0, temperature T, and cross-section σ_{lim}:

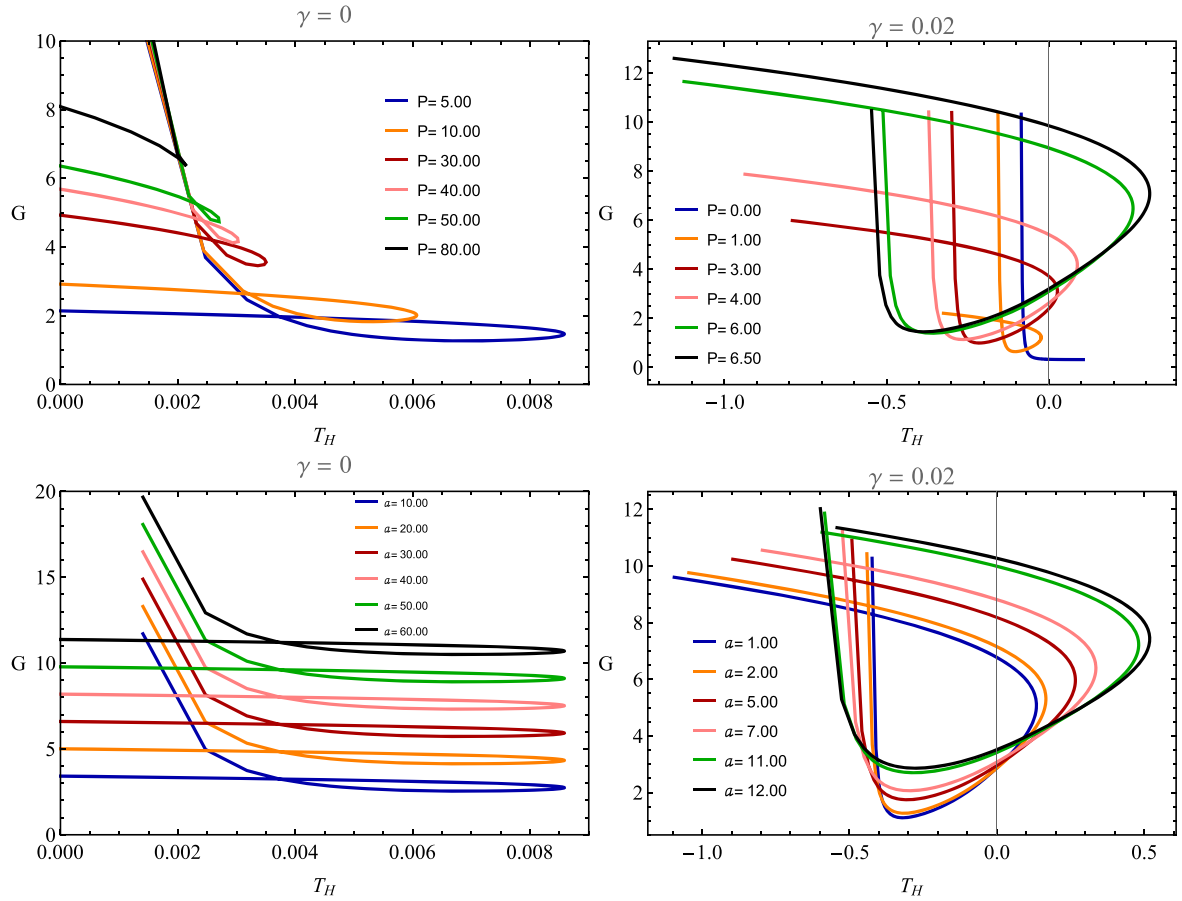

Figure 7. Gibbs free energy G. Values of fixed parameters are $M = 0.002,\ P = 5.0,\ a = 2.0$.

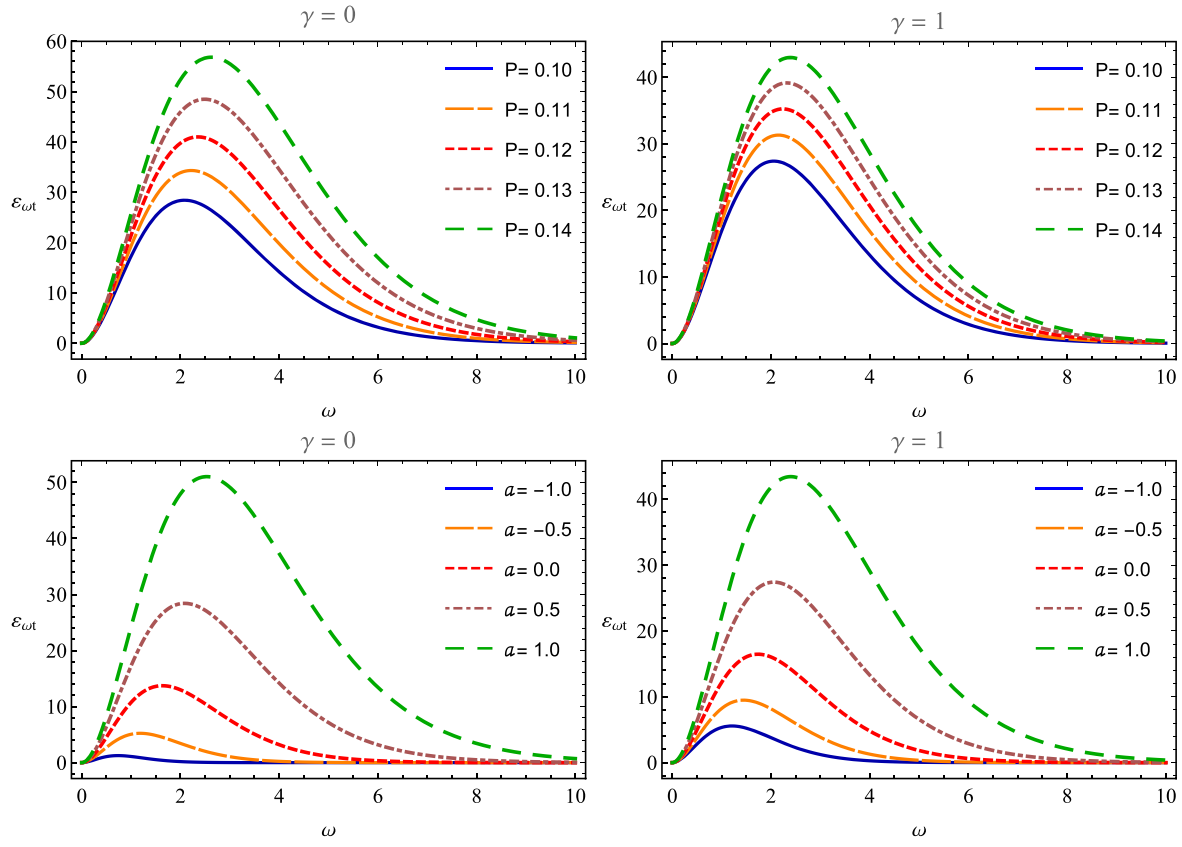

Figure 8. Emission energy $\varepsilon_{\omega t}$. Values of fixed parameters are $P = 0.10,\ a = 0.5$.

$$\frac{\mathrm{d}^2\varepsilon}{\mathrm{d}\omega \mathrm{d}t} = (2\pi^3 r_0^2)\omega^3 \left[\exp\left[\omega \right.\right. \times \left[\frac{-24\gamma P \log\left(\frac{(4a\sqrt{r_0^2} + 24\pi P r_0^2 + 1)^2}{16\pi} \right) + 24\pi P r_0^2 + 1}{4\sqrt{\pi}\sqrt{\pi r_0^2 - \gamma \log\left(\frac{(4a\sqrt{r_0^2} + 24\pi P r_0^2 + 1)^2}{16\pi} \right)}} \right. \left.\left. + \frac{a}{\pi} \right]^{-1} \right] - 1 \left.\right]^{-1}. \quad (29)$$

One can obtain information about emission energy from figure 8. One can see that $\varepsilon_{\omega t}$ increases with increasing values of P & a for both large and small BHs. Moreover $\varepsilon_{\omega t}|_{\gamma=0} > \varepsilon_{\omega t}|_{\gamma=1}$.

7. Conclusion

In our current analysis, we delve into the study of a new type of BH solution called the Rindler–Schwarzschild BH, which is differentiated through the parameters a from the Schwarzschild BH solution. When $a = 0$, the solution corresponds to the original Schwarzschild BH. It is important to note that the Rindler–Schwarzschild BH is thermodynamically stable. We consider the pressure $P = -\frac{1}{8\pi}\Lambda$. We investigate the thermal stability of the solution by analyzing its temperature and heat capacity, as well as its phase transition via heat capacity and Gibbs free energy analysis, thermal fluctuations, and mass evaporation through energy emission by comparing the small and large BHs and also the results with the Schwarzschild BH by setting $a = 0$.

Our study shows that the positive behavior of the metric function $f(r)$ and mass M ensure the physical existence of Rindler–Schwarzschild BHs. The temperature $T > 0$ predicts the physical existence of the solutions, and $C_P > 0$ ensures the thermally stable hairy BHs. As decay is natural in realistic objects, the evaporation of mass is predicted through the energy emission process. Every realistic object undergoes a transitional phase while turning from an unstable to a stable state, as evidenced by the swallowing behaviors of Gibbs free energy and transmission of heat capacity from negative to positive region. The critical points for phase transition are apparent in heat capacity dissipation.

In the domain of a very short event horizon, we observe the monotonically increasing behavior of entropy in the case of small BHs and negative pressure P. The height of entropy decreases for a specific value of the radii, which signifies an abrupt change and represents a thermal fluctuation in the system. We also find that small BHs ($0 < \gamma \leqslant 1$) are more affected by thermal fluctuations. Whereas no fluctuation process occurs in the case of positive P and larger black holes ($\gamma = 0$). Furthermore, Rindler–Schwarzschild BHs exhibit natural evaporation. In summary, this study has physical significance in predicting the existence of realistic small and large Rindler–Schwarzschild BHs.

Acknowledgments

The paper was funded by the National Natural Science Foundation of China 11975145. AÖ would like to acknowledge the contribution of the COST Action CA21106—COSMIC WISPers in the Dark Universe: Theory, astrophysics and experiments (CosmicWISPers) and the CA22113—Fundamental challenges in theoretical physics (THEORY-CHALLENGES). We also thank the Scientific and Technological Research Institution of Turkey (TUBITAK) and the Sponsoring Consortium for Open Access Publishing in Particle Physics (or SCOAP3) for their support.

Conflict of interest statement

The authors declare that they have no known competing financial interests or personal relationships that could have appeared to influence the work reported in this paper.

ORCID iDs

Allah Ditta https://orcid.org/0000-0001-7758-8736

References

[1] Bekenstein J D 1973 Black holes and entropy *Phys. Rev.* D **7** 2333
[2] Bekenstein J D 1974 Generalized second law of thermodynamics in black holephysics *Phys. Rev.* D **9** 3292
[3] Hawking S W 1975 Particle creation by black holes *Commun. Math. Phys.* **43** 199
[4] Vagnozzi S *et al* 2023 Horizon-scale tests of gravity theories and fundamental physics from the Event Horizon Telescope image of Sagittarius A *Class. Quantum Grav.* **40** 165007
[5] Gibbons G W and Hawking S W 1977 Action integrals and partition functions inquantum gravity *Phys. Rev.* D **15** 2752
[6] Bardeen J M, Carter B and Hawking S W 1973 The Four laws of black hole mechanics *Commun. Math. Phys.* **31** 161
[7] Teitelboim C 1985 The cosmological constant as a thermodynamic black hole parameter *Phys. Lett.* B **159** 293
[8] Kastor D, Ray S and Traschen J 2009 Enthalpy and the mechanics of AdS black holes *Class. Quantum Grav.* **26** 195011
[9] Dolan B P 2011 The cosmological constant and the black hole equation of state *Class. Quantum Grav.* **28** 125020
[10] Kuang X M, Liu B and Övgün A 2018 Nonlinear electrodynamics AdS black hole and related phenomena in the extended thermodynamics *Eur. Phys. J.* C **78** 840
[11] Dolan B P 2001 Pressure and volume in the first law of black hole thermodynamics *Class. Quantum Grav.* **28** 235017
[12] Kubiznak D and Mann R B 2012 P-V criticality of charged AdS black holes *J. High Energy Phys.* JHEP07(2012)033

[13] Israel W and Khan K A 1964 Collinear particles and bondi dipoles in general relativity *Nuovo Cim.* **33** 331
[14] Aryal M, Ford L and Vilenkin A 1986 Cosmic strings and black holes *Phys. Rev.* D **34** 2263
[15] Achucarro A, Gregory R and Kuijken K 1995 Abelian Higgs hair for black holes *Phys. Rev.* D **52** 5729
[16] Gregory R, Kubiznak D and Wills D 2013 Rotating black hole hair *J. High Energy Phys.* JHEP06(2013)023
[17] Kinnersley W and Walker M 1970 Uniformly accelerating charged mass in general relativity *Phys. Rev.* D **2** 1359
[18] Plebanski J F and Demianski M 1976 Rotating, charged, and uniformlyaccelerating mass in general relativity *Ann. Phys.* **98** 98
[19] Gregory R and Hindmarsh M 1995 Smooth metrics for snapping strings *Phys. Rev.* D **52** 5598
[20] Anabalón A, Appels M, Gregory R, Kubizňák D, Mann R B and Ovgün A 2018 Holographic thermodynamics of accelerating black holes *Phys. Rev.* D **98** 104038
[21] Bonjour F, Emparan R and Gregory R 1999 Vortices and extreme black holes: the Question of flux expulsion *Phys. Rev.* D **59** 084022
[22] Martinez E A and York J W Jr 1990 Thermodynamics of black holes and cosmic strings *Phys. Rev.* D **42** 3580
[23] Costa M S and Perry M J 2000 Interacting black holes *Nucl. Phys.* B **591** 469
[24] Dutta K, Ray S and Traschen J 2006 Boost mass and the mechanics of accelerated blackholes *Class. Quantum Grav.* **23** 335
[25] Herdeiro C, Kleihaus B, Kunz J and Radu E 2010 On the Bekenstein-Hawking area law for black objects with conical singularities *Phys. Rev.* D **81** 064013
[26] Krtous P and Zelnikov A 2020 Thermodynamics of two black holes *J. High Energy Phys.* JHEP02(2020)164
[27] Ramirez-Valdez C J, Garcia-Compean H and Manko V S 2020 Thermodynamics of two aligned Kerr black holes *Phys. Rev.* D **102** 024084
[28] Hawking S W and Page D N 1983 Thermodynamics of black holes in anti-de Sitter space *Commun. Math. Phys.* **87** 577
[29] Pourhassan B and Faizal M 2015 Thermal fluctuations in a charged AdS black hole *Europhys. Lett.* **111** 40006
[30] Pourhassan B, Upadhyay S, Saadat H and Farahani H 2018 Quantum gravity effects on HoravaLifshitz black hole *Nucl. Phys.* B **928** 415
[31] Pourhassan B and Faizal M 2016 Thermodynamics of a sufficient small singly spinning Kerr-AdS black hole *Nucl. Phys.* B **913** 834
[32] Faizal M and Khalil M M 2015 GUP-corrected thermodynamics for all black objects and the existence of remnants *Int. J. Mod. Phys.* A **30** 1550144
[33] Kaul R K and Majumdar P 2000 Logarithmic correction to the Bekenstein-Hawking entropy *Phys. Rev. Lett.* **84** 5255
[34] Carlip S 2000 Logarithmic corrections to black hole entropy from the Cardy formula *Class. Quantum Grav.* **17** 4175
[35] Zhang M 2018 Corrected thermodynamics and geometrothermodynamics for anti-de Sitter black hole *Nucl. Phys.* B **935** 170
[36] Pourhassan B, Faizal M and Debnath U 2016 Effects of thermal fluctuations on the thermodynamics of modified Hayward black hole *Eur. Phys. J.* C **76** 145
[37] Bargueno P, Contreras E and Rincon A 2021 Thermodynamics of scale-dependent Friedmann equations *Eur. Phys. J.* C **81** 477
[38] Wald R M 1984 *General Relativity* (Chicago, IL: University of Chicago)
[39] Grumiller D, Kummer W and Vassilevich D V 2002 Dilaton gravity in two dimensions *Phys. Rep.* **369** 327
[40] Berger B K, Chitre D M, Moncrief V E and Nutku Y 1972 Hamiltonian Formulation of Spherically Symmetric Gravitational Fields *Phys. Rev.* D **5** 2467
[41] Russo J G and Tseytlin A A 1992 Scalar-tensor quantum gravity in two dimensions *Nucl. Phys.* B **382** 259
[42] Odintsov S D and Shapiro I L 1991 One-loop renormalization of two-dimensional induced quantum gravity *Phys. Lett.* B **263** 183
[43] Grumiller D 2010 Model for gravity at large distances *Phys. Rev. Lett.* **105** 211303
[44] Talmadge C, Berthias J P, Hellings R W and Standish E M 1988 Model-independent constraints on possible modifications of Newtonian gravity *Phys. Rev. Lett.* **61** 1159
[45] Mandal S, Das S, Gogoi D J and Pramanik A 2023 Leading-order corrections to the thermodynamics of Rindler modified Schwarzschild black hole *Phys. Dark Univ.* **42** 101349
[46] Sakalli I and Ovgun A 2017 Hawking radiation and deflection of light from Rindler modified Schwarzschild black hole *Europhys. Lett.* **118** 60006
[47] Halilsoy M, Gurtug O and Mazharimousavi S H 2013 Rindler modified Schwarzschild geodesics *Gen. Relativ. Gravit.* **45** 2363
[48] Ali R, Tiecheng X and Babar R 2024 First-order quantum corrections of tunneling radiation in modified Schwarzschild-Rindler black hole *Gen. Relativ. Gravit.* **56** 13
[49] Sakalli I and Mirekhtiary S F 2014 Spectroscopy of Rindler modified Schwarzschild black hole *Astrophys. Space Sci.* **350** 727
[50] Dolan B P 2011 Pressure and volume in the first law of blackhole thermodynamics *Class. Quantum Grav.* **28** 235017
[51] Samart D and Channuie P 2023 AdS to dS phase transition mediated by thermalon in Einstein-Gauss-Bonnet gravity from Renyi statistics *Nuc. Phys.* B **989** 116140
[52] Ashtekar A and Magnon A 1984 Asymptotically anti-de Sitterspace-times *Class. Quantum Grav.* **1** L39
[53] Ashtekar A and Das S 2000 Asymptotically anti-de Sitter spacetimes: conserved quantities *Class. Quantum Grav.* **17** L17
[54] Das S and Mann R 2000 Conserved quantities in Kerr-anti-deSitter space-times in various dimensions *J. High Energy Phys.* JHEP08(2000)033
[55] Gong T F, Jiang J and Zhang M 2023 Holographic thermodynamics of rotating black holes *J. High Energy Phys.* JHEP06(2023)105
[56] Ma M S and Zhao R 2014 Corrected form of the first law of thermodynamics for regular black holes *Class. Quantum Grav.* **31** 245014
[57] Dolan B P 2011 Pressure and volume in the first law of black hole thermodynamics *Class. Quantum Grav.* **28** 235017
[58] Feng H, Huang Y, Hong W and Tao J 2021 Charged torus-like black holes as heat engines *Commun. Theor. Phys.* **73** 045403
[59] Ali R and Asgher M 2022 Tunneling analysis under the influences of Einstein-Gauss-Bonnet black holes gravity theory *New Astron.* **93** 101759
[60] Ali R, Babar R and Asgher M 2022 Gravitational analysis of rotating charged black-hole-like solution in Einstein-Gauss-Bonnet gravity *Ann. Phys.* **534** 2200074
[61] Pourhassan B and Faizal M 2015 Thermal fluctuations in a charged AdS black hole *Europhys. Lett.* **111** 40006
[62] Gibbons G W, Hawking S W and Perry J M 1978 Path integrals and the indefiniteness of the gravitational action *Nucl. Phys.* B **138** 141
[63] Hartle J B and Hawking S W 1976 Path-integral derivation of black-hole radiance *Phys. Rev.* D **13** 2188
[64] Sobreiro R F and Otoya V J V 2007 Effective gravity from a quantum gauge theory in Euclidean spacetime *Class. Quantum Grav.* **24** 4937
[65] Bonora L and Bytsenko A A 2011 Partition functions for quantum gravity, black holes, elliptic genera and Lie algebra homologies *Nucl. Phys.* B **852** 508

[66] Akhtar Z, Babar R and Ali R 2023 Thermal fluctuations evolution of the new Schwarzschild black hole *Ann. Phys.* **448** 169190
[67] Gibbons G W and Hawking S W 1977 Action integrals and partition functions in quantum gravity *Phys. Rev.* D **15** 2752
[68] Iyer V and Wald R M 1995 Comparison of the Noether charge and Euclidean methods for computing the entropy of stationary black holes *Phys. Rev.* D **52** 4430
[69] Govindarajan T R, Kaul R K and Suneeta V 2001 Logarithmic correction to the Bekenstein-Hawking entropy of the BTZ black hole *Class. Quantum Grav.* **18** 2877
[70] Das S, Majumdar P and Bhaduri R K 2002 General logarithmic corrections to black-hole entropy *Class. Quantum Grav.* **19** 2355
[71] Sadeghi J, Pourhassan B and Rahimi F 2014 Logarithmic corrections of charged hairy black holes in, (2+ 1) dimensions *Canad. J. Phys.* **92** 1638
[72] Ma M S and Zhao R 2014 Corrected form of the first law of ther-modynamics for regular black holes *Class. Quantum Grav.* **31** 245014
[73] Mo J X, Li G Q and Xu X B 2016 Combined effects of f, (R) gravity and conformally invariant Maxwell field on the extended phase space thermodynamics of higher-dimensional black holes *Eur. Phys. J.* C **76** 1
[74] Cai R G, Cao L M, Li L and Yang R Q 2013 PV criticality in the extended phase space of Gauss-Bonnet black holes in AdS space *J. High Energy Phys.* JHEP09(2013)005
[75] Cai R G, Hu Y P, Pan Q Y and Zhang Y L 2015 Thermodynamics of black holes in massive gravity *Phys. Rev.* D **91** 024032
[76] Akhtar Z, Khan A, Ahmad Z and Ali R 2023 Study of first-order corrections and phase transition of RN de-sitter black hole *New Astron.* **98** 101936
[77] Sadeghi J, Pourhassan B and Rostami M 2016 P- V criticality of logarithm-corrected dyonic charged AdS black holes *Phys. Rev.* D **94** 064006
[78] Yang S J, Zhou R, Wei S W and Liu Y X 2022 Kinetics of a phase transition for a Kerr-AdS black hole on the free-energy landscape *Phys. Rev.* D **105** 084030
[79] Javed W, Ali R, Babar R and Övgün A 2019 Tunneling of massive vector particles from types of BTZ-likeblack holes *Eur. Phys. J. Plus* **134** 511
[80] Övgün A, Javed W and Ali R 2018 Tunneling Glashow-Weinberg-Salam model particles from black hole solutions in Rastall theory *Adv. High Energy Phys.* **2018** 3131620
[81] Javed W, Abbas G and Ali R 2017 Charged vector particle tunneling from a pair of accelerating and rotating and 5D gauged super-gravity black holes *Eur. Phys. J.* C **77** 296
[82] Javed W, Ali R and Abbas G 2019 Charged vector particles tunneling from 5D black hole and black ring *Can. J. Phys.* **97** 176
[83] Javed W, Ali R, Babar R and Övgün A 2020 Tunneling of massive vector particles under the influence of quantum gravity *Chin. Phys.* C **44** 015104
[84] Ditta A, Tiecheng X, Mustafa G, Yasir M and Atamurotov F 2022 Thermal stability with emission energy and Joule-Thomson expansion of regular BTZ-like black hole *Eur. Phys. J.* C **82** 756
[85] Ditta A, Tiecheng X, Ali R, Atamurotov F, Mahmood A and Mumtaz S 2023 Thermodynamic stability of the regular charged torus-like black hole *Ann. Phys.* **453** 169326
[86] Ditta A, Tiecheng X, Ali R and Mustafa G 2023 Thermal stability and tunneling radiation in Van der Waals black hole *Nucl. Phys.* B **994** 116287
[87] Anabalón A, Appels M, Gregory R, Kubizňák D, Mann R B and Ovgün A 2018 Holographic Thermodynamics of Accelerating Black Holes *Phys. Rev.* D **98** 104038
[88] Ali R, Bamba K and Ali S S A 2019 Effect of quantum gravity on the stability of black holes *Symmetry* **11** 631
[89] Ali R, Asgher M and Malik F M 2020 Gravitational analysis of neutral regular black hole in Rastall gravity *Mod. Phys. Lett.* A **35** 2050225
[90] Mirekhtiary S F, Sakalli I and Bashiry V 2021 Fermion tunneling, instability, and first law of Rindler modified Schwarzschild black hole as a thermodynamic system *Can. J. Phys.* **99** 118–24
[91] Ali R, Babar R, Akhtar Z and Övgün A 2023 Thermodynamics and logarithmic corrections of symmergent black holes *Results Phys.* **46** 106300